Nonlinear quantum dynamics at a classical second-order resonance

S. Dyrting and G. J. Milburn
Department of Physics, University of Queensland, St. Lucia, Queensland 4072, Australia

C. A. Holmes
Department of Mathematics, University of Queensland, St. Lucia, Queensland 4072, Australia
(Received 1 March 1993)

We compare the classical and quantum-mechanical motion of a distribution initially localized on a classical second-order resonance of a driven pendulum. As the driving is increased the quantum state becomes localized about the classically stable region of phase space. The existence of a parity symmetry then allows for coherent tunneling between isolated second-order resonances. We compare and contrast the classical and quantum behavior with the aid of perturbation theory.

PACS number(s): 05.45.+b, 42.50.Vk

I. INTRODUCTION

The concept of a resonance is central to an understanding of the dynamics of driven Hamiltonian systems. In the study of classical chaos the complicated topology of trajectories can be explained by the formation and interaction of resonances at successively finer scales. In particular, a resonance can lead to the emergence of a locally stable region of phase space which may persist even after surrounding trajectories have become chaotic and a distribution of points contained within such a region will remain localized.

In this paper we are interested in the formation of stable regions in quantum-mechanical phase space and the motion of wave packets initially confined near such regions. A lot of theoretical and numerical work has been done by Berman and co-workers [1–3] and Lin and Reichl [4] on quantum systems containing many energy levels resonant with a periodic driving force. Under certain conditions these free-energy levels will be trapped. That is, if the initial state of the perturbed system is an energy eigenstate of the free system, with energy in the resonance zone, the dynamics will not mix in free-energy states beyond the resonance zone. This is analogous to the trapping of classical trajectories by KAM surfaces. Other researchers [5–7] have studied the rate of tunneling of quantum wave packets between resonances of a bistable system. They have found that tunneling can be enhanced or suppressed by periodic driving. In this paper we will study the dynamic localization of a wave packet initially situated on a classical second-order resonance. For our numerical work we have chosen a nonlinear pendulum perturbed by a periodic modulation of its linearized frequency. This system is essentially different from those used to study tunneling because the free dynamics has only one stable fixed point. Bistability arises as a consequence of the modulation and the parity symmetry of the Hamiltonian.

In our system a freely evolving wave packet will quickly become delocalized because of the nonlinear frequency of the pendulum. We also observe revivals of the initial wave packet which can be explained in terms of the local nonlinearity of the classical oscillator [8]. As the amplitude of the frequency modulation increases from zero we find that both the classical phase-space distribution and the quantum-mechanical wave packet become localized about the classical second-order resonance. The dynamic phase-space localization of a classical distribution can be explained by the increase in width of the classical resonance. We explain dynamic phase-space localization in the quantized motion by showing that as the perturbation is increased certain quasistationary states have Q functions that become peaked about the stable classical fixed points. To explain the change in the quantum-mechanical Q functions we generalize normal time-independent quantum perturbation theory to include perturbations periodic in time. This is done by introducing the notion of an extended Hilbert space, a technique already used in quantum stability theory [9]. We show that resonances in second-order classical perturbation theory imply near-resonant denominators at second order in time-dependent quantum perturbation theory. As a result perturbed quasistationary states rapidly develop support on near-resonant free states, and it is the interference between these states which causes the change in topography of the Q function. Once the classical distribution has become localized we find that a further increase in the perturbation strength causes the classical region of stable motion to shrink and the distribution to become delocalized. In the corresponding quantum-mechanical evolution we find that the wave packet begins to tunnel between resonances. We interpret this behavior in terms of the presence of a parity symmetry and the gradual detuning of the dominant quasifrequencies.

The layout of this paper is as follows. In Sec. II we introduce the models to be discussed, both classical and quantum mechanical. In Sec. III we describe the structure of classical phase space with the aid of classical perturbation theory and introduce our generalization of time-independent quantum perturbation theory. The results of numerical simulations and their interpretation in terms of quantum perturbation theory are given in

Sec. IV. A discussion of results and further topics of research is presented in Sec. V.

II. THE DRIVEN PENDULUM

The states of a classical pendulum are represented by an angle coordinate q restricted to the interval $[-\pi,\pi)$ and an angular momentum p. The evolution of a pendulum corresponds to the motion of q and p in phase space. The pendulum which we consider is

$$H(t)=\frac{p^2}{2}-\kappa(1-2\epsilon\cos\Omega t)\cos q. \tag{2.1}$$

When $\epsilon=0$ Eq. (2.1) reduces to the ordinary time-independent nonlinear pendulum. This Hamiltonian has a single stable fixed point at $(q,p)=(0,0)$ and exhibits bounded motion inside the cosine potential well and unbounded motion over the top of the cosine potential. The frequency of the motion linearized about $(q,p)=(0,0)$ is equal to $\sqrt{\kappa(1-2\epsilon\cos\Omega t)}$ and so (2.1) corresponds to a pendulum with a modulating linearized frequency. Equation (2.1) also describes the center-of-mass motion of a two-level atom in an electromagnetic standing wave in the limit of large atom-field detuning [10]. For this case q would be the position of the atom and p its linear momentum. In this case the time-dependent coupling could be produced by modulating the field frequency at a frequency Ω.

For the case $\epsilon=0$ the total energy $E=\frac{p^2}{2}-\kappa\cos q$ is a constant of the motion and the classical mechanics is exactly integrable. For nonzero ϵ the coupling of the driving term with the integrable motion of the free nonlinear pendulum leads to a modification of the invariant and in the case of a classical resonance a change in the topology of phase-space orbits. The overlap of resonances leads to the formation of a layer of stochastic motion about the classical separatrix. The resonances that do not overlap persist as stable regions of phase space.

The classical stroboscopic dynamics of the variables q and p are determined by the recursive formula

$$(q',p')=F((q,p))=(\bar{q}(q,p,T),\bar{p}(q,p,T)), \tag{2.2}$$

where $T=2\pi/\Omega$ is the period of the driving term and the functions $\bar{q}(q,p,t)$ and $\bar{p}(q,p,t)$ are determined by Hamilton's equations

$$\frac{d\bar{q}}{dt}=\bar{p}, \tag{2.3a}$$

$$\frac{d\bar{p}}{dt}=-\kappa(1-2\epsilon\cos\Omega t)\sin\bar{q}, \tag{2.3b}$$

and the initial conditions $\bar{q}(q,p,0)=q$ and $\bar{p}(q,p,0)=p$. The map F possesses the two important symmetries,

$$FP=PF, \tag{2.4a}$$

$$FT=TF^{-1}. \tag{2.4b}$$

Here P: $(q,p)\mapsto(-q,-p)$ denotes the parity transformation and T: $(q,p)\mapsto(q,-p)$ denotes the time-reversal reflection about the q axis. Henceforth we fix $\kappa=1.2$ and study the stroboscopic dynamics as ϵ is increased. In Fig. 1 we show the classical stroboscopic phase portraits for $\epsilon=0.0,0.1,0.2$, and 0.3. To generate these pictures we have taken as initial conditions points lying along the p axis and applied the map F 500 times. As a consequence of the symmetries P and T the stroboscopic portraits remain unchanged by reflections about either axis. When $\epsilon=0.1$ a layer of stochastic motion has already formed about the separatrix. Elliptic fixed points are evident about the regions $(q,p)\approx(0,0)$, $(q,p)\approx(0,\pm1.2)$, and $(q,p)\approx(0,\pm2.2)$. Note that the stable regions centered on $(q,p)\approx(0,\pm1.2)$ increase in area as ϵ increases from 0.0 to 0.2 and begin to decrease when ϵ is increased to 0.3.

When the mean height of the cosine potential κ is of the same order as the quantum energy spacing at the bottom of the cosine well $\hbar\sqrt{\kappa}$ then quantum-mechanical effects become significant. The Hamiltonian for the quantum pendulum is generated from Eq. (2.1) by replacing the real variables q and p by Hermitian operators $\hat{q}$ and $\hat{p}$ satisfying the commutation relation $[\hat{q},\hat{p}]=i\hbar$. The Hamiltonian $\hat{H}(t)$ acts on the Hilbert space $\mathcal{H}$ of states spanned by the $\hat{p}$ eigenstates $|n\rangle$ such that $\hat{p}|n\rangle=\hbar n|n\rangle$. If $\hat{q}$ and $\hat{p}$ were the operators of position and linear momentum n would be any real number. For simplicity we choose $\hat{q}$ and $\hat{p}$ to be the operators of angle and angular momentum. For this case n is an integer. The quantum analog of the iterative map Eq. (2.2) is the evolution operator

$$\hat{F}=\hat{U}(T), \tag{2.5}$$

where $\hat{U}(t)$ is the unitary evolution operator generated by $\hat{H}(t)$ via the differential equation

$$i\hbar\frac{d\hat{U}(t)}{dt}=\hat{H}(t)\hat{U}(t). \tag{2.6}$$

The orthonormal eigenstates of $\hat{F}$ denoted by $|w_m\rangle$ for $m=0,1,2,\ldots$ which satisfy

$$\hat{F}|w_m\rangle=\exp(-iw_mT)|w_m\rangle \tag{2.7}$$

provide a convenient basis for studying the stroboscopic evolution. An arbitrary state

$$|\psi\rangle=\sum_{m=0}^{\infty}|w_m\rangle\langle w_m|\psi\rangle \tag{2.8}$$

evolves to

$$\hat{F}^n|\psi\rangle=\sum_{n=0}^{\infty}\exp(-inw_mT)|w_m\rangle\langle w_m|\psi\rangle \tag{2.9}$$

after n cycles of the driving term. The analogues of the classical symmetries Eq. (2.4a) and Eq. (2.4b) are

$$\hat{F}\hat{P}=\hat{P}\hat{F}, \tag{2.10a}$$

$$\hat{F}\hat{T}=\hat{T}\hat{F}^{-1}, \tag{2.10b}$$

where $\hat{P}$ is the linear parity operator with the following

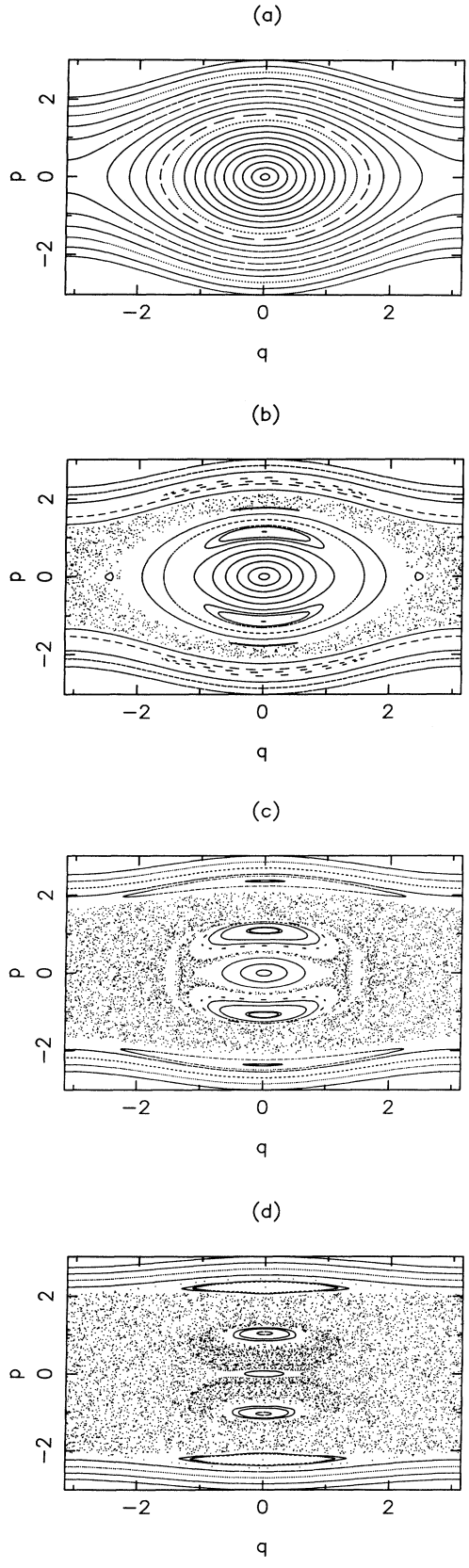

FIG. 1. Plot of classical stroboscopic phase-space portraits. (a) $\epsilon = 0.0$, (b) $\epsilon = 0.1$, (c) $\epsilon = 0.2$, (d) $\epsilon = 0.3$.

action on momentum eigenstates:

$$\hat{P}|n\rangle = |-n\rangle. \tag{2.11}$$

$\hat{T}$ is the antilinear time-reversal operator with the same action as $\hat{P}$ on the momentum eigenstates. As $\hat{P}$ commutes with $\hat{F}$ and $\hat{P}^2 = \hat{1}$ the states $|w_m\rangle$ are even or odd parity under $\hat{P}$,

$$\hat{P}|w_m\rangle = \pm|w_m\rangle. \tag{2.12}$$

Expanding $|w_m\rangle$ in terms of momentum eigenstates

$$|w_m\rangle = \sum_{n=-\infty}^{\infty} |n\rangle\langle n|w_m\rangle, \tag{2.13}$$

it follows from Eqs. (2.7) and (2.10b) and the antilinearity of $\hat{T}$ that

$$\hat{F}\hat{T}|w_m\rangle = \exp(-iw_m T)\hat{T}|w_m\rangle. \tag{2.14}$$

Thus $|w_m\rangle$ and $\hat{T}|w_m\rangle$ are degenerate. We may now form a new basis of quasistationary states by symmetric and antisymmetric combinations of degenerate pairs. In that case as the parity condition implies $\langle n|\omega_m\rangle = \pm\langle n|\omega_m\rangle^*$ the expansion of the new quasistationary states in the momentum basis may then be chosen real. This property is useful in the numerical diagonalisation of $\hat{F}$.

III. PERTURBATION THEORY

A. Classical

A thorough discussion of classical perturbation theory can be found in [11]. Here we present a summary of as much of the formalism as will be required in subsequent sections.

Denote the nonlinear pendulum (2.1) in the limit $\epsilon = 0$ by H_0. As noted in Sec. II the existence of a constant of the motion ensures that the dynamics generated by the Hamiltonian is integrable. By this we mean that there is a canonical transformation from (q, p) to new conjugate variables (I, θ) such that H_0 is a function of I only and the classical frequency of oscillation $\omega_{\rm cl}(I)$ is

$$\omega_{\rm cl}(I) = \frac{d\theta}{dt} = \frac{dH_0(I)}{dI}. \tag{3.1}$$

Consider the perturbation of the Hamiltonian, Eq. (2.1), as a power series in ϵ,

$$H(I, \theta, t) = H_0(I) + \epsilon H_1(I, \theta, t), \tag{3.2}$$

where $H_1 = 2\kappa \cos(\Omega t) \sin(q)$. To determine if first-order resonances occur we Fourier analyze the first-order (in ϵ) term, i.e., $\epsilon H_1(I, \theta, t)$,

$$H_1 = \sum_{m=0,\ \pm1,\ \pm2,\ldots} H_{1,2m}[\exp i(\Omega t + 2m\theta) + \text{c.c.}]. \tag{3.3}$$

Then first-order resonance solutions occur for I given by

$$2m\omega_{\rm cl}(I) - \Omega = 0, \quad m = 0, \pm 1, \pm 2, \ldots \quad . \tag{3.4}$$

To determine if second-order resonances occur we must first find approximate action angle variables $(\bar{I}, \bar{\theta})$ for $H(I, \theta, t)$ up to and including the order-ϵ terms. Provided I is not close to a first-order resonance, we can do this through a canonical transformation so that the new Hamiltonian is

$$\bar{H}(\bar{I}, \bar{\theta}, t) = H_0(\bar{I}) + \epsilon^2 H_2(\bar{I}, \bar{\theta}, t) + \cdots \quad . \tag{3.5}$$

There are two things to note here. Firstly, there is no order-ϵ term. This is because H_1 is purely oscillatory. Up to order ϵ then the only qualitative changes introduced by the perturbation are due to the first-order resonances. Secondly, the canonical transformation has introduced an ϵ^2 term into the new Hamiltonian, $\epsilon^2 H_2$. It is the Fourier analysis of this term that shows the second-order resonance solutions. Here

$$H_2 = \sum_{m=0, \pm 1, \pm 2} H_{2,2m}[\exp i(2\Omega t + 2m\theta) + \text{c.c.}] + (\text{time-independent terms}). \tag{3.6}$$

So second-order resonances occur for $\bar{I}$ given by

$$m\omega_{\rm cl}(\bar{I}) - \Omega = 0, \quad m = 0, \pm 1, \pm 2, \ldots \quad . \tag{3.7}$$

If I (or $\bar{I}$) satisfies a resonance condition it is not an approximate invariant as in an integrable system. In fact it can be shown that a chain of stable and unstable orbits lie in its place. Further, there is a region around the stable periodic orbits in which solutions lie on tori, or invariant curves for the stroboscopic map. We can calculate the width, perpendicular to the invariant I of this region, as an estimate of the size of the resonance. For first-order resonances the width is of order $\sqrt{\epsilon}$ and for second order of order ϵ. So for ϵ small first-order resonances are typically more important. However, for the system we have here all the first-order resonances are clustered near the separatrix. For $\epsilon = 0.1$ they have overlapped to form a chaotic band as seen in Fig. 1(b). But there is one second-order resonance $\omega_{\rm cl}(\bar{I}) = \pm\Omega$ at a significantly smaller value of $\bar{I}$ which is important. The two stable periodic points that replace the invariant appear in Fig. 1(b) as fixed points of the stroboscopic map at $(q, p) \approx (0.0 \pm 1.2)$ and the width of the resonance is surprisingly large ≈ 0.44. The calculation of the positions and widths of the resonances is given in the Appendix.

B. Quantum

In Sec. III A we saw how classical perturbation theory could describe the structure of phase space for systems perturbed slightly away from the integrable Hamiltonian H_0. In this section we aim to develop the formalism of quantum perturbation theory as a means of describing quantum phase space for the quantized driven pendulum.

Some of the formalism described below has already appeared in the context of quantum stability [9]. Dinaberg and Sinai [12] and Craig [13] have developed an operator KAM theory in close analogy with the Lie-transformation method as it applies to the classical KAM theorem. As we shall see, the perturbation theory developed below is analogous to the classical theory discussed in Sec. III A.

We begin with the observation that in the limit of $\epsilon = 0$ the quantum stroboscopic map $\hat{F}$ is simply

$$\hat{F} = \exp\left(\frac{-i\hat{H}_0 T}{\hbar}\right), \tag{3.8}$$

where $\hat{H}_0$ is the quantized nonlinear pendulum. Denote the stationary states of $\hat{H}_0$ with energy $\hbar\omega_m$ by $|\omega_m\rangle$, then $|\omega_m\rangle$ is a quasistationary state for $\hat{F}$ with quasifrequency $w_m = \omega_m$. In analogy with time-independent quantum perturbation theory we assume that for small ϵ the perturbed quasistationary states $|w_m\rangle$ and quasifrequency w_m are close to $|\omega_m\rangle$ and ω_m, respectively, and then attempt to find corresponding asymptotic expansions.

Let $|w_m(t)\rangle$ denote the state evolving from the initial quasistationary state $|w_m\rangle$ under the time-dependent dynamics (2.6) generated by the Hamiltonian

$$\hat{H}(t) = \hat{H}_0 + \epsilon\hat{H}_1(t). \tag{3.9}$$

For the moment consider the general case where $\hat{H}_1(t)$ is any Hermitian operator periodic in time with fundamental frequency Ω. Then $|w_m(t)\rangle$ satisfies the time-dependent Schrödinger equation

$$i\hbar\frac{d}{dt}|w_m(t)\rangle = \hat{H}(t)|w_m(t)\rangle, \tag{3.10}$$

subject to the quasiperiodicity condition

$$|w_m(T)\rangle = \exp(-iw_m T)|w_m(0)\rangle. \tag{3.11}$$

We introduce states $|v_m\rangle$ periodic in t

$$|v_m\rangle = \exp(iw_m t)|w_m(t)\rangle. \tag{3.12}$$

Then $|v_m\rangle$ satisfies the equation

$$\hbar w_m|v_m\rangle = -i\hbar\frac{d}{dt}|v_m\rangle + \hat{H}(t)|v_m\rangle. \tag{3.13}$$

In order to use the methods of time-independent perturbation theory we introduce the notion of an extended Hilbert space as follows. Since $|v_m\rangle$ is periodic in t it has a Fourier expansion in terms of the momentum eigenstates $|n\rangle$ and time,

$$|v_m\rangle = \sum_{l,n=-\infty}^{\infty} \exp(i\Omega l t)v_{mln}|n\rangle. \tag{3.14}$$

We can think of the function $\exp(i\Omega l t)$ as an eigenstate of the "momentum" operator

$$\hat{h} = -i\hbar\frac{d}{dt} \tag{3.15}$$

in the Hilbert space $L_2(0, T)$. Denote this state by $|l\rangle$. Equation (3.14) is now thought of as an expansion of $|v_m\rangle$

in terms of the states $|n,l\rangle = |n\rangle \otimes |l\rangle$ and Eq. (3.13) becomes an eigenvalue problem

$$\hbar w_m |v_m\rangle = \hat{K}|v_m\rangle, \tag{3.16}$$

where $\hat{K}$ is the Hermitian operator

$$\hat{K} = \hat{h} + \hat{H}(\hat{t}) \tag{3.17}$$

acting on the extended Hilbert space $\mathcal{K} = \mathcal{H} \otimes L_2(0,T)$.

Once the eigenvalue problem Eq. (3.16) has been solved we can recover the quasistationary state $|w_m\rangle$ by the projection

$$|w_m\rangle = \langle t=0|v_m\rangle, \tag{3.18}$$

where

$$|t\rangle = \sum_{l=-\infty}^{\infty} |l\rangle \exp(i\Omega l t). \tag{3.19}$$

To solve the eigenvalue problem perturbatively we diagonalize the "free" operator

$$\hat{K}_0 = \hat{h} + \hat{H}_0. \tag{3.20}$$

The eigenstates of $\hat{K}_0$ are just $|\omega_m, l\rangle = |\omega_m\rangle \otimes |l\rangle$ and it is not difficult to verify that

$$\hat{K}_0 |\omega_m, l\rangle = \hbar(\omega_m + l\Omega)|\omega_m, l\rangle, \tag{3.21}$$

so that $|\omega_m, l\rangle$ has the eigenvalue $\hbar(\omega_m + l\Omega)$. Without a loss of generality we look for eigenstates of $\hat{K}$ that reduce to $|\omega_m, 0\rangle$ in the limit as ϵ vanishes. We assume that the energy level $\hbar\omega_m$ of $\hat{K}$ is nondegenerate and that $|v_m\rangle$ and w_m have the following asymptotic expansions:

$$w_m = \omega_m + \epsilon w_m^{(1)} + \epsilon^2 w_m^{(2)} + O(\epsilon^3), \tag{3.22a}$$

$$|v_m\rangle = |\omega_m, 0\rangle + \epsilon|v_m^{(1)}\rangle + \epsilon^2|v_m^{(2)}\rangle + O(\epsilon^3). \tag{3.22b}$$

The new quasifrequency and quasistationary state are then calculated using standard Rayleigh-Schrödinger perturbation theory [14]. Up to second-order the corrections to the quasifrequencies are

$$\hbar w_m^{(1)} = \langle \omega_m | \hat{H}_{10} | \omega_m \rangle, \tag{3.23a}$$

$$\hbar w_m^{(2)} = \left\langle \omega_m \middle| \sum_l \hat{H}_{1l}^\dagger \frac{1}{\hbar\omega_m - \hat{H}_0 - \hbar l\Omega} \times (1 - \delta_{l0}\hat{P}_m)\hat{H}_{1l} \middle| \omega_m \right\rangle, \tag{3.23b}$$

and setting all arbitrary constants to zero before projecting onto $\mathcal{H}$ the corrections to the quasistationary state are

$$|w_m^{(1)}\rangle = \hat{A}_m^{(1)}|\omega_m\rangle, \tag{3.24a}$$

$$|w_m^{(2)}\rangle = \hat{A}_m^{(2)}|\omega_m\rangle, \tag{3.24b}$$

where

$$\hat{A}_m^{(1)} = \sum_l \frac{1}{\hbar\omega_m - \hat{H}_0 - \hbar l\Omega}(1 - \delta_{l0}\hat{P}_m)\hat{H}_{1l}, \tag{3.25a}$$

$$\hat{A}_m^{(2)} = -\sum_k \frac{1}{\hbar\omega_m - \hat{H}_0 - \hbar k\Omega}(1 - \delta_{k0}\hat{P}_m) \times \left(\hbar w_m^{(1)} \frac{1}{\hbar\omega_m - \hat{H}_0 - \hbar k\Omega}(1 - \delta_{k0}\hat{P}_m)\hat{H}_{1k} - \sum_l \hat{H}_{1l}^\dagger \frac{1}{\hbar\omega_m - \hat{H}_0 - \hbar(k-l)\Omega}(1 - \delta_{kl}\hat{P}_m)\hat{H}_{1k-l} \right). \tag{3.25b}$$

In the above equations $\hat{P}_m = |\omega_m\rangle\langle\omega_m|$ denotes the projection onto $|\omega_m\rangle$ and $\hat{H}_{1l}$ is the Fourier component of $\hat{H}_1$ rotating at frequency $l\Omega$. Equations (3.23a) to (3.25b) are the natural generalization of perturbation theory to the case of perturbations periodic in time. By setting $\hat{H}_l = \hat{0}$ for all $l \neq 0$ we recover the expressions of normal time-independent perturbation theory [14]. Note that the time-dependent components of $\hat{H}_1(t)$ only begin to contribute to the shift in quasifrequency at second order. This is analogous to the result that to first order in ϵ the classical Hamiltonian $\bar{H}(\bar{I})$ only depends on the cycle-averaged part of $H(t)$ [11].

The matrix elements $\langle\omega_{m'}|\hat{A}_m^{(1)}|\omega_m\rangle$ and $\langle\omega_{m'}|\hat{A}_m^{(2)}|\omega_m\rangle$ become singular when the free-energy levels satisfy the resonance condition

$$\hbar(\omega_m - \omega_{m'}) = \hbar l\Omega, \tag{3.26}$$

where l is an integer. We will call them first- or second-order resonances, depending at which order the singularity occurs. In the language of time-independent perturbation theory and extended Hilbert space a quantum resonance indicates that the Hamiltonian K_0 has degenerate energy levels. In this case we must use degenerate perturbation theory to find the new quasistationary states.

There is an important difference between the classical and quantum-mechanical perturbation theories outlined above: Exact quantum resonances are less likely than classical resonances because quantum frequencies are discrete whilst classical frequencies form a continuum.

If the system is semiclassical, by which we mean that the principal of quantized action gives a good approximation to the quantum energy levels of the free Hamiltonian $\hat{H}_0$, then for nearby energy levels the local classical frequency is related to the energy difference by the equation [15]

$$\omega_m - \omega_{m-n} \approx n\omega_{\rm cl}(I_m), \tag{3.27}$$

where I_m is the semiclassical action. For each classical

resonance $n\omega_{\rm cl} - l\Omega = 0$ there will be energy levels $\hbar\omega_m$ and $\hbar\omega_{m-n}$ satisfying the near-resonance condition

$$\hbar(\omega_m - \omega_{m-n}) \approx \hbar l\Omega. \tag{3.28}$$

The perturbed quasistationary state $|w_m\rangle$ will rapidly develop a significant component along $|\omega_{m-n}\rangle$ as ϵ is increased. In the work by Berman and co-workers [1–3,16] and in our following analysis it is assumed that the free-energy spacing is well approximated by a low-order expansion in the principal quantum number n. When this is not the case we would expect there to be quantum resonances that are not present in the classical model.

Now consider the special case (2.1) where $\hat{H}_1(t) = 2\kappa\cos(\Omega t)\cos(\hat{q})$. For the classical second-order resonance where $n = l = \pm 2$ there will be energy levels satisfying

$$\hbar(\omega_m - \omega_{m\mp 2}) \approx \pm 2\hbar\Omega. \tag{3.29}$$

We see from Eq. (3.25b) that these states give rise to near-resonant denominators in the second-order of quantum perturbation theory.

IV. RESULTS

In this section we present the results of numerical studies of the dynamics of the Hamiltonian Eq. (2.1) in both its classical and quantized forms. We study the change in the classical evolution of an ensemble of 1000 points as the perturbation ϵ is increased from 0.0 to 0.3. The points are initially centered near the second-order resonance $(q,p) \approx (0.0, 1.2)$ with density

$$Q(q,p) = \frac{1}{2\pi\sqrt{\sigma_q\sigma_p}} \exp\left(\frac{(p-\bar{p})^2}{2\sigma_p}\right) \exp\left(\frac{(q-\bar{q})^2}{2\sigma_q}\right). \tag{4.1}$$

This is a bivariate Gaussian centered on $(\bar{q},\bar{p})$ with angle and momentum variances σ_q and σ_p, respectively. To investigate the quantum dynamics we use the Q function as the appropriate analog of the classical phase-space distribution. A quantum state $|\psi\rangle$ will define a probability density on classical phase space by

$$Q(q,p) = \frac{1}{2\pi\hbar}|\langle q,p|\psi\rangle|^2. \tag{4.2}$$

The states $|q,p\rangle$ are coherent states for a simple harmonic oscillator with frequency $\sqrt{\kappa}$.

A. Classical

In Fig. 2 we have plotted the momentum mean $\langle p\rangle$ and variance $V(p)$ as a function of the strobe number n for a cloud of 1000 points evolving under the classical dynamics Eq. (2.2). The points have an initial density given by Eq. (4.1) with means $(\bar{q},\bar{p}) = (0.0, 1.0)$ with variances $\sigma_q = 0.084$ and $\sigma_p = 0.036$. For these simulations we have taken $\kappa = 1.2$ and $\Omega = 1$.

When $\epsilon = 0.0$ we see that the mean momentum quickly drops to zero and the momentum variance rises as the

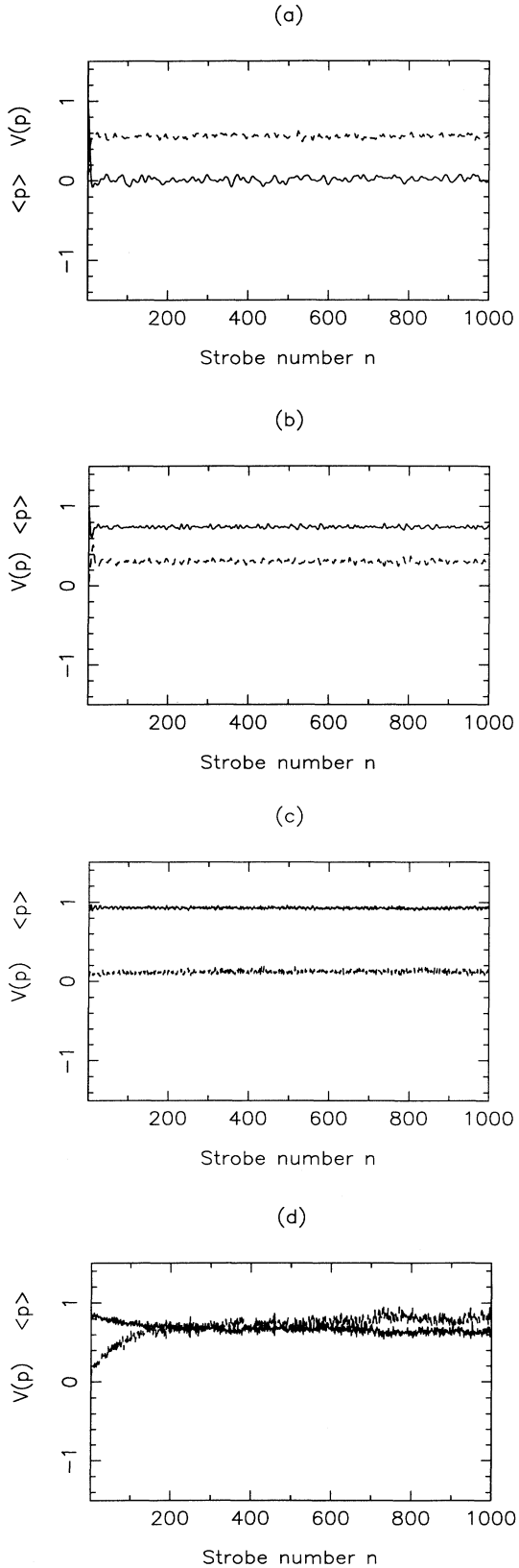

FIG. 2. Plot of classical momentum statistics vs n. (a) $\epsilon = 0.0$, (b) $\epsilon = 0.1$, (c) $\epsilon = 0.2$, (d) $\epsilon = 0.3$. Solid line, $\langle p\rangle$; dashed line, $V(p)$.

classical distribution is smeared out over the trajectories of constant energy. This delocalization is due to the nonlinear dependence of the free Hamiltonian on the action. As the perturbation parameter ϵ is increased from 0.0 to 0.2 the growth in momentum variance is suppressed and the mean momentum remains near its initial value, indicating that the classical distribution is being localized about the stable fixed point. We interpret this as follows. The width of the stable region is increasing linearly with ϵ until the classical distribution is contained within the region of the elliptic fixed point. As noted in Sec. III A when ϵ is increased to 0.3 the stable region of phase space begins to shrink because of the destruction of KAM tori. As a result we see in Fig. 2(d) that the classical distribution becomes delocalized again.

B. Quantum

In our simulations of the quantum dynamics of Eq. (2.1) we have taken $\hbar = 0.05$. The Floquet operator $\hat{U}(T)$ was found by numerically integrating the operator differential equation (2.6) in the momentum representation. Since $\hat{P}$ and $\hat{T}$ are symmetries of the quantum evolution and the quasistationary states are real in the momentum basis the problem of finding eigenstates of $\hat{U}(T)$ reduces to the diagonalization of a real symmetric matrix. The stationary states $|\omega_m\rangle$ and the energies $\hbar\omega_m$ were found by diagonalizing the Hamiltonian (2.2) in the momentum representation and are labeled in order of increasing energy.

We have graphed the quantum mean $\langle\hat{p}\rangle$ and variance $V(\hat{p})$ of momentum as a function of the strobe number n in Fig. 3. The initial state $|\psi\rangle$ was chosen to be a minimum uncertainty state with $\langle\hat{q}\rangle = 0.0$, $\langle\hat{p}\rangle = 1.0$, and $\langle\Delta\hat{p}^2\rangle = 0.01$ so that its Q function was equal to the classical probability distribution (4.1). Once the Floquet operator had been diagonalized we used Eq. (2.9) to calculate the quantum stroboscopic evolution. When $\epsilon = 0.0$ we see that initially the mean momentum quickly drops to zero and the momentum variance rises as the quantum wave packet becomes delocalized. This is due to the nonlinear dependence of ω_m on the quantum number m. The decrease in momentum variance when n is a multiple of 150 indicates a revival of the initial wave packet and can be explained by a quadratic dependence of ω_m on m [8].

Like the classical dynamics of a distribution of points we find that as ϵ increases from 0.0 to 0.2 the growth in the quantum momentum variance is suppressed and the mean becomes fixed about its initial value, indicating that the state is being localized. In Fig. 4 we have represented the probability distribution of the state $|\psi\rangle$ in the $\epsilon = 0.0$ and $\epsilon = 0.2$ bases of quasistationary states. The length of each phasor χ_m equals the overlap probability $|\langle w_m|\psi\rangle|^2$ and its angle equals the eigenphase $-w_m T$. Comparing the two distributions we see that as the perturbation parameter is increased the support on the quasistationary states has decreased to two states with almost identical quasifrequencies. We have verified that these states have opposite parity and for the purpose of

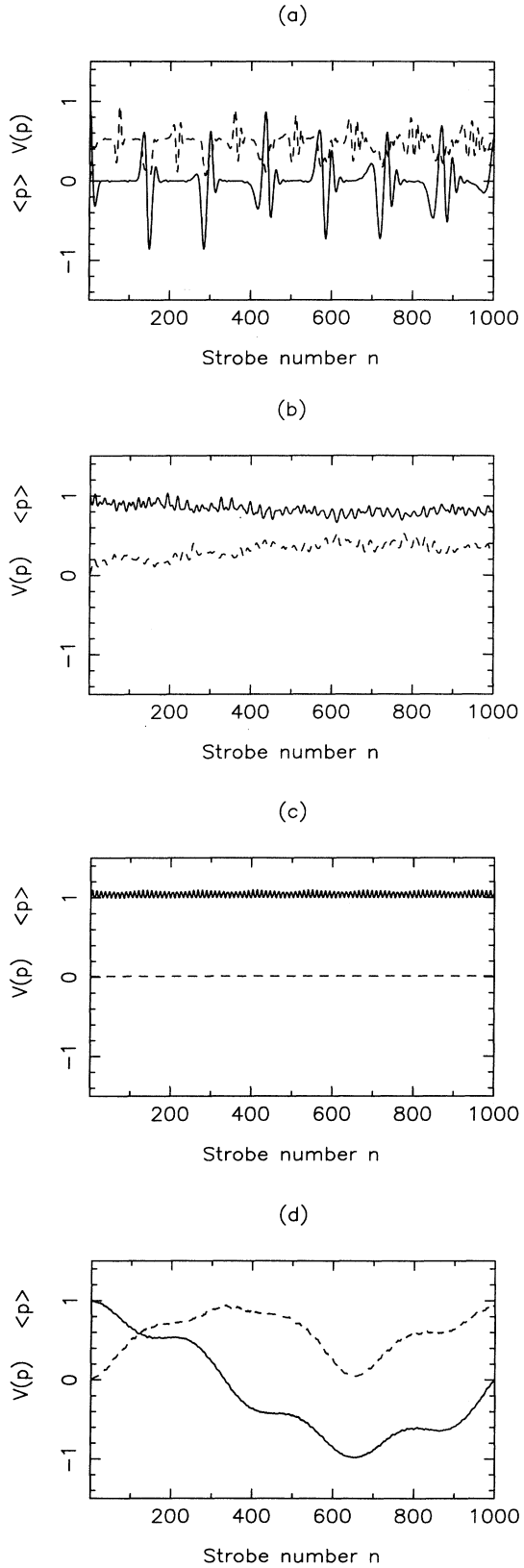

FIG. 3. Plot of quantum momentum statistics vs n. (a) $\epsilon = 0.0$, (b) $\epsilon = 0.1$, (c) $\epsilon = 0.2$, (d) $\epsilon = 0.3$. Solid line, $\langle\hat{p}\rangle$; dashed line, $V(\hat{p})$.

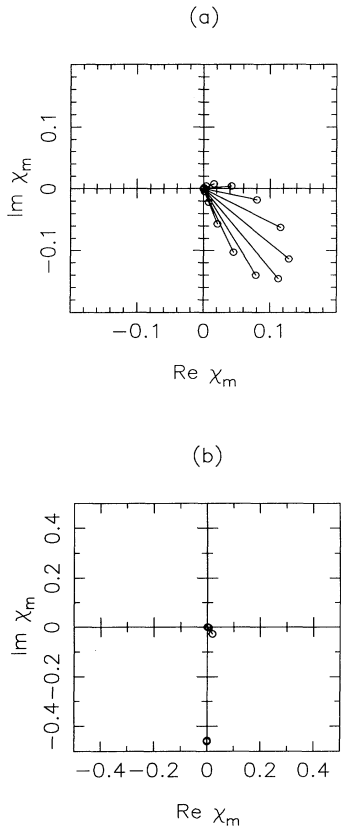

FIG. 4. Quasistationary state distribution of minimum uncertainty state. (a) $\epsilon = 0.0$, (b) $\epsilon = 0.2$.

this discussion $|w_+\rangle$ and $|w_-\rangle$ will denote the even and odd states respectively.

In Fig. 5 we have expanded $|w_-\rangle$ in terms of the unperturbed stationary states $|\omega_m\rangle$. We find that it is a superposition of a dominant state $|\omega_{12}\rangle$ and two other states $|\omega_{10}\rangle$ and $|\omega_{14}\rangle$ satisfying the near-resonant conditions

$$\hbar(\omega_{12} - \omega_{10}) = 0.103 \approx 2\hbar\Omega, \tag{4.3}$$

$$\hbar(\omega_{12} - \omega_{14}) = -0.101 \approx -2\hbar\Omega. \tag{4.4}$$

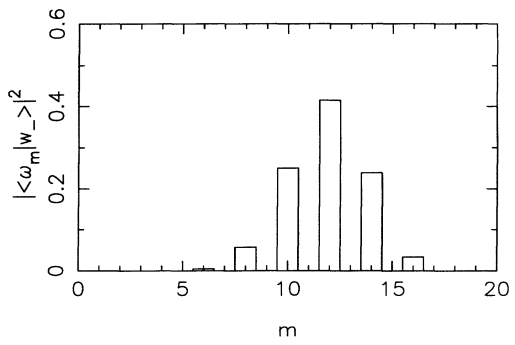

FIG. 5. Expansion of perturbed eigenstate $|w_-\rangle$ for $\epsilon = 0.2$.

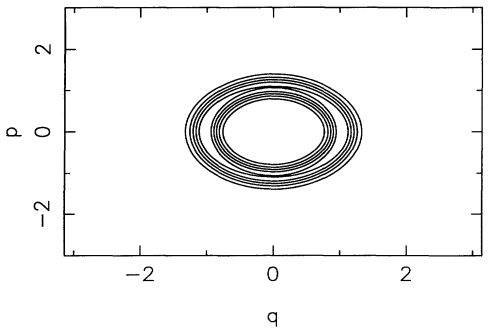

FIG. 6. Q function of stationary state $|\omega_{12}\rangle$.

As noted in Sec. III B these energy levels give rise to small denominators in second-order quantum perturbation theory. To see the effect of the second-order quantum resonance on the phase-space distribution of a quasistationary state we have plotted the Q functions for the dominant state $|\omega_{12}\rangle$ and $|w_-\rangle$ in Figs. 6 and 7, respectively. As expected we find that the Q function of $|\omega_{12}\rangle$ is concentrated about an ellipse corresponding to an orbit of the free pendulum. But we find that the phase-space density of $|w_-\rangle$ is very different. Evidently the interference between near-resonant states has caused the Q function in Fig. 7 to become concentrated about the stable regions of the classical second-order resonance. Now we see the role of the quantum resonance in the dynamic localization of quantum wave packets. It has caused the resonant quasistationary states to become strongly peaked about the stable fixed points such that the initial minimum uncertainty state is approximated by a sum of two states with opposite parity. Since these two states have almost identical quasifrequencies the minimum uncertainty is approximately stationary.

When ϵ is increased to 0.3 we would expect the quantum motion to reflect the delocalization of the classical distribution shown in Fig. 2(d). Since the minimum uncertainty state is the sum of two quasistationary states with opposite parity we would expect to find coherent tunneling between the region $(q,p) \approx (0.0, 1.2)$ and its reflected partner $(q,p) \approx (0.0, -1.2)$. This is precisely what we see in Fig. 3(d) and is due to the detuning of the two dominant quasifrequencies.

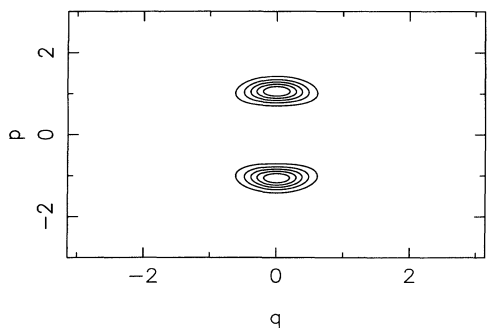

FIG. 7. Q function of quasistationary state $|w_-\rangle$ for $\epsilon = 0.2$.

V. DISCUSSION

We have studied the quantum dynamics of a state initially concentrated near a classical second-order resonance of a driven pendulum. In the absence of driving the state undergoes a sequence of delocalizations followed by revivals. This is due to the nonlinearity of the free pendulum. As the driving strength increases the state becomes localized, a result reflecting the change in topography of the underlying quasistationary states. The concentration of the quasistationary state's Q function can be explained by the interference of near-resonant stationary states, a result predicted by second-order quantum perturbation theory. After the minimum uncertainty state collapses to a sum of two quasistationary states we see coherent tunneling between the stable regions of the classical resonance.

In this paper we have stressed that the localization we observe occurs because of a second-order resonance in quantum perturbation theory and is analogous to the localization of a classical distribution at a classical second-order resonance. But we would expect from the results of Sec. III that localization and tunneling will occur at first-order resonances as well. Indeed, since the small denominators occur at lower order in ϵ the localization should develop faster than for second-order resonances.

We have not studied the effect on dynamic localization of varying the driving frequency Ω, but quantum perturbation theory predicts we should observe the following behavior. Firstly, as Ω is increased from zero we would expect that resonance stuctures should develop first amongst separatrix eigenstates because their quasifrequencies are more closely spaced than for low-lying states. Secondly, if the driving is changed so that the difference in quantum number n of the resonating states is increased, we would expect that the perturbed quasistationary states would generate more complicated Q functions so that a minimum uncertainty state located on a resonance might no longer be well approximated by two states with opposite parity.

In this paper we have studied the effects of quantum resonances on quasistationary states. But quantum perturbation theory can also be used to study the change in quasifrequencies. In particular, Eqs. (3.23a) and (3.23b) suggest that the tunneling rate for driven bistable systems should be linear or quadratic depending on the nature of the perturbation. This would merit further study.

APPENDIX

Here we give details of the first- and second-order resonances, of the classical system. Starting with the action for the nonlinear pendulum

$$I(H_0)=\frac{8\sqrt{\kappa}}{\pi}\left[\mathcal{E}\left(\frac{\pi}{2};N\right)-(1-N^2)\mathcal{F}\left(\frac{\pi}{2};N\right)\right], \quad \text{(A1)}$$

where $N^2=(H_0+\kappa)/2\kappa$, $\mathcal{F}$ is the elliptic integral of the first kind, $\mathcal{E}$ is the elliptic integral of the second kind, and the classical frequency of oscillation is then

$$\omega_{\rm cl}(H_0)=\frac{\pi}{2}\frac{\sqrt{\kappa}}{\mathcal{F}(\frac{\pi}{2};N)}. \quad \text{(A2)}$$

First-order resonances occur for [see (3.4)]

$$\mathcal{F}\left(\frac{\pi}{2};N\right)=\frac{\pi\sqrt{\kappa}}{\Omega}m, \quad m=0,\pm1,\pm2,\ldots. \quad \text{(A3)}$$

In particular, if $\Omega=1$, $\kappa=1.2$, and $m=1$, then $H_0=1.15$ and the stroboscopic map has a fixed point at $(q,p)\approx(0,2.2)$.

Using the fact that the angle for the nonlinear pendulum is

$$\theta(H_0,q)=\frac{\pi}{2}\frac{\mathcal{F}(\xi;N)}{\mathcal{F}(\frac{\pi}{2};N)}, \quad \text{(A4)}$$

where $N\sin\xi=\sin q/2$, we can write the perturbation $H_1=2\kappa\cos\Omega t\cos q$ as a function of θ and H_0 and expand as a Fourier series in θ. See Eq. (3.3). The first few amplitudes are

$$H_{10}=\kappa\left[1-\frac{4\pi^2}{K^2}\left(\frac{Q}{(1-Q)^2}+\frac{Q^3}{(1-Q^3)^2}+\ldots\right)\right], \quad \text{(A5)}$$

$$H_{12}=\frac{2\kappa\pi^2}{K^2}\left(\frac{Q}{(1-Q)^2}-\frac{2Q^2}{(1-Q)(1-Q^3)}-\frac{2Q^4}{(1-Q^3)(1-Q^5)}-\cdots\right), \quad \text{(A6)}$$

$$H_{14}=\frac{4\kappa\pi^2}{K^2}\left(\frac{Q^2}{(1-Q)(1-Q^3)}-\frac{Q^3}{(1-Q)(1-Q^5)}-\ldots\right), \quad \text{(A7)}$$

where $Q=\exp(-\pi K'/K)$, $K=\mathcal{F}(\frac{\pi}{2};N)$, and $K'=\mathcal{F}(\frac{\pi}{2};\sqrt{1-N^2})$.

We now attempt a canonical transformation to action-angle variables $(\bar{I},\bar{\theta})$ for $H(I,\theta,t)$ up to and including the order-ϵ terms. This we do through a generating function, $\theta\bar{I}+W(\theta,\bar{I},t)$, where

$$W(\theta,\bar{I},t)=\epsilon W^{(1)}(\theta,\bar{I},t)+\epsilon^2W^{(2)}(\theta,\bar{I},t)+\cdots, \quad \text{(A8)}$$

such that the new action-angle variables are given by

$$\bar{\theta}=\theta+\frac{\partial W}{\partial I}, \quad \text{(A9)}$$

$$I=\bar{I}+\frac{\partial W}{\partial\theta}, \quad \text{(A10)}$$

and the new Hamiltonian is

$$\bar{H}=H+\frac{\partial W}{\partial t}. \quad \text{(A11)}$$

Choosing $W^{(1)}$ such that $\bar{H}$ is a function of $\bar{I}$ only (up to order ϵ) gives

$$W^{(1)}=\sum_{m=0,\pm1,\pm2,\ldots}\frac{iH_{1,2m}}{2m\omega_{\rm cl}(\bar{I})-\Omega}[\exp i(\Omega t+2m\theta)+\text{c.c.}]. \quad \text{(A12)}$$

However, $W^{(1)}$ becomes singular if the first-order resonance condition (3.4) holds, clearly indicating that $\bar{I}$ is not an approximate invariant there.

To investigate a first-order resonance, say that furthest from the separatrix at $m = 1$, consider I close to the resonance condition. Then remove all the other first-order resonances through the canonical transformation given above without the $m = 1$ term. The new Hamiltonian is then

$$\bar{H}(\bar{I}, \bar{\theta}, t) = H_0(\bar{I}) + 2\epsilon H_{12} \cos(\Omega t + 2\bar{\theta}) + O(\epsilon^2), \quad \text{(A13)}$$

valid in the neighborhood of the resonance. Transforming to a rotating frame we find the equations are approximately those of the nonlinear pendulum. The width of the resonance is defined as the width of the separatrix of this pendulum,

$$\sqrt{\frac{2\epsilon H_{1,2}}{d\omega_{cl}/dI}}. \quad \text{(A14)}$$

For $\Omega = 1$, $\kappa = 1.2$, and $\epsilon = 0.1$ the width ≈ 0.43 and the resonances have overlapped with the separatrix itself.

Second-order resonances arise because through the canonical transformation given above the new Hamiltonian $\bar{H}$ [Eq. (3.5)] has a term second order in ϵ; $\epsilon^2 H_2$, where

$$H_2 = \frac{1}{2}\left(\frac{\partial W^{(1)}(\bar{I}, \bar{\theta}, t)}{\partial \theta}\right)^2 \frac{\partial^2 H_0(\bar{I})}{\partial I^2} + \sum_m \frac{\partial W^{(1)}}{\partial \theta} H_{1,2m}[\exp i(\Omega t + 2m\theta) + \text{c.c.}]. \quad \text{(A15)}$$

The Fourier analysis of H_2, see Eq. (3.6), shows that resonances occur for $\bar{I}$ given by $m\omega_{cl}(\bar{I}) + \Omega = 0$, $m = 0, \pm 1, \pm 2, \ldots$, and, in particular, for $\bar{I}$ given by $\omega_{\rm cl}(\bar{I}) \pm \Omega = 0$. For $\Omega = 1$, $\kappa = 1.2$ this means the stroboscopic map has stable fixed points at $(q, p) \approx (0.0, \pm 1.2)$. We can analyze this resonance exactly as we did for the first-order resonance. The width is given by

$$\epsilon\sqrt{\frac{2H_{2,2}}{d\omega_{\rm cl}(\bar{I})/dI}}, \quad \text{(A16)}$$

which for $\Omega = 1$, $\kappa = 1.2$, and $\epsilon = 0.1$ is ≈ 0.44.

[1] G.P. Berman and G.M. Zaslavsky, Phys. Lett. **61A**, 295 (1977).

[2] G.P. Berman, G.M. Zaslavsky, and A.R. Kolovsky, Phys. Lett. **87A**, 152 (1982).

[3] G.P. Berman and A.R. Kolovsky, Phys. Lett. **95A**, 15 (1983).

[4] W.A. Lin and L.E. Reichl, Phys. Rev. A **40**, 1055 (1989).

[5] F. Grossman, P. Jung, T. Dittrich, and P. Hänggi, Z. Phys. B **84**, 315 (1991).

[6] F. Grossman, P. Jung, T. Dittrich, and P. Hänggi, Phys. Rev. Lett. **67**, 516 (1991).

[7] W.A. Lin and L.E. Ballentine, Phys. Rev. Lett. **65**, 2927 (1990).

[8] S. Dyrting and G.J. Milburn, Phys. Rev. A **47**, R2484 (1993).

[9] J. S. Holland, in *SCHRÖDINGER OPERATORS: The Quantum Many-Body Problem*, edited by. E. Baslev (Springer, Berlin, 1992).

[10] M.J. Holland, D.F. Walls, and P. Zoller, Phys. Rev. Lett. **67**, 1716 (1991).

[11] A. Lichtenberg and M. Lieberman, *Regular and Stochastic Motion* (Springer, New York, 1983).

[12] E. I. Dinaberg and Ya. Sinai, Func. Anal. Appl. **9**, 279 (1985).

[13] W. Craig, Commun. Math. Phys. **88**, 113 (1983).

[14] E. Merzbacher, *Quantum Mechanics* (Wiley, New York, 1970).

[15] I.Sh. Averbukh and N.F. Perelman, Phys. Lett. **139**, 449 (1989).

[16] G.P. Berman and A.R. Kolovsky, Physica D **8**, 117 (1983).